I&EC research
Industrial & Engineering Chemistry Research

pubs.acs.org/IECR

Article

Optimizing the Packing Density and Chemistry of Cellulose Nanofilters for High-Efficiency Particulate Removal

Shao-Hsiang Hung, Jared W. Bowden, Richard E. Peltier, and Jessica D. Schiffman*

Cite This: https://doi.org/10.1021/acs.iecr.1c03051

Read Online

ACCESS | Metrics & More | Article Recommendations | Supporting Information

ABSTRACT: The global spread of COVID-19 as well as the worsening air pollution throughout the world have brought tremendous attention to the development of materials that can efficiently capture particulate matter. We suggest that the high porosity of electrospun filters composed of nanofibers could provide minimal obstruction to air flow, while their high tortuosity and surface area-to-volume ratio present an excellent platform to capture particulates. In this study, the removal of nanoscale particles via in-house fabricated cellulose nanofilters is significantly enhanced by chemically functionalizing the fibers' surface via the deposition of the bioinspired glue polydopamine (PDA) or the polycation poly(diallyldimethylammonium chloride) (PDADMAC). The effects of filter packing density, layering thickness, and chemistry on their performance, i.e., their filtration efficiency, most penetrating particle size (MPPS), particle fractional penetration percent, and performance in a high relative humidity environment, were investigated. When evaluated in an extremely hazardous environment (PM concentration ~ 2000 $\mu g\ m^{-3}$), the filtration efficiency, pressure drop, and quality factor for the cellulose nanofilters were measured to be >98.0%, <200 Pa, and ~0.03 Pa^{-1}, respectively. When we evaluated the performance of a composite hydrophobic/hydrophilic filter in an 80% relative humidity environment, a 99.8% filtration efficiency was achieved. We have demonstrated that the removal of nanoscale particulates can be effectively captured using cellulose-based nanofilters, even in a nonideal high humidity environment. These fundamental investigations into the structure−property-chemistry relationships of in-house electrospun nanofilters on nanoscale particulate removal hold the potential to help drive the future engineering of nanofilters for air purification applications, which is a timely and extremely important concern.

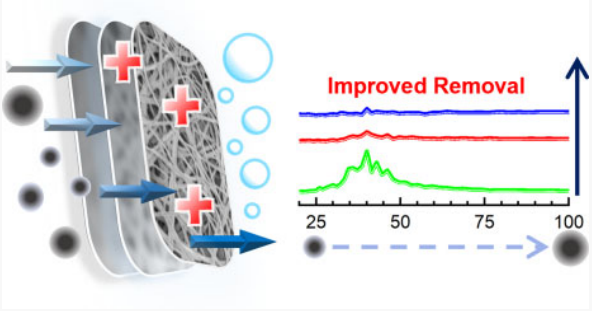

INTRODUCTION

According to the World Health Organization (WHO), ~91% of the world's population is breathing polluted air, and more than 8 million deaths annually are caused by ambient and household air pollution.[1,2] Additionally, to date, the global spread of the Severe Acute Respiratory Syndrome Coronavirus-2 (SARS-CoV-2) has caused ~200 million reported cases of COVID-19 and 4 million deaths.[3,4] The urgent need for air filters, as well as face masks, has brought tremendous attention to the development of efficient filtration technologies.[5]

Filters are a promising technology to reduce human exposure to particulate matter (PM) and especially to particulates that have an aerodynamic diameter smaller than 2.5 μm ($PM_{2.5}$), which pose the greatest threat to human health. Studies have shown that $PM_{2.5}$ can easily penetrate into human lungs and the bloodstream and that long-term exposure to $PM_{2.5}$ increases both morbidity and mortality.[2,6−8] $PM_{2.5}$ chemical components include inorganic matter (SiO_2, SO_4^{2-}, NO_3^-), organic matter (elemental carbon, carbon black), bacteria, and viruses, that result from diverse sources, such as diesel engine combustion, soil dust, coal, and agricultural field burning.[9] Unfortunately, with the exception of N95 respirators, most common filters, composed of fabric, glass fibers, or melt blown fibers, exhibit low efficiency at removing these submicrometer and nanoscale particles, especially in nonideal environments, such as high temperature and high humidity.[10,11] While it is possible to improve the particle removal efficiency by using a thicker filter, this results in a trade-off of having a larger pressure drop and increased energy consumption.[10]

Electrospinning is a simple, scalable, and well-studied technique for producing randomly accumulated nano- and microscale diameter fibers.[10,12,13] The manufactured fiber meshes have a large surface-to-volume ratio and high porosity, which can be used as filters for aerosol[14−17] and particulate matter removal applications.[18−24] Previously, numerous researchers have explored the effect of fiber morphology (i.e., uniform fiber, beaded fiber, composite fiber) and nanofiber

Received: July 29, 2021
Revised: October 8, 2021
Accepted: October 10, 2021

chemistry on filtration quality factors (QFs).[14,17,24−26] Additionally, the structure−property relationships between electrospun filters and their filtration efficiency (E, see eq 1) have been studied by relating four physical parameters, fiber diameter, filter thickness (Z), basis weight (W, see eq 2), and packing density (α, see eq 3), to filter performance, such as quality factor (QF, see eq 4).[14,27−31] In eq 1, C_{up} and C_{down} are the number of particle counts at the filter upstream and downstream, respectively, whereas in eq 3, ρ_f is the density of the filter material. In eq 4, ΔP is the pressure drop across the filter.

$$E = 1 - \frac{C_{down}}{C_{up}} \tag{1}$$

$$W = \frac{\text{filter mass}}{\text{filter area}} \tag{2}$$

$$\alpha = \frac{W}{\rho_f Z} \tag{3}$$

$$\text{QF} = \frac{\ln(1 - E)}{\Delta P} \tag{4}$$

For example, when Leung et al.[27] investigated the relationship between the basis weight, filter thickness, and packing density on the filtration efficiency of poly(ethylene oxide) nanofibers, they found that the filtration efficiency increased with basis weight, while the most penetrating particle size (MPPS) decreased with increasing packing density. In a different study, featuring nylon nanofibers,[29] it was determined that the filtration efficiency was positively associated with filter thickness and negatively associated with fiber diameter. However, there was no clear correlation between packing density and filtration efficiency. Furthermore, since most existing air filters identify a MPPS at around 300 nm, recent studies have focused on the removal of $PM_{1.0}$ and even $PM_{0.1}$ to further evaluate filter performance.[30−32] For instance, both Liu et al.[31] and Chen et al.[32] were able to manipulate polymer solution phase separation to fabricate nanofiber/net filters with a decreased pore size and increased surface potential. This enabled the electropsun nanofilters to have an improved ability to remove particles less than one micron with a minimal pressure drop, while also providing their light structure and greater optical transmittance.

Here, we systematically investigated the structure−property relationships of in-house electrospun nanofibers on filtration performance. The base nanofilter chemistry selected for this work was cellulose because it is sustainable and commonly used in environmental applications.[33] By controlling the filter thickness, we investigated the relationship between the filter packing density and the overall filter performance. Also, previous literature does not commonly discuss the MPPS and particle size fractional penetration (P%). Here we investigated this parameter to further evaluate its importance in the ability of the nanofilters to remove < $PM_{1.0}$ (i.e., particulate ranging from 20 to 900 nm). Cellulose's affinity for further chemical modification is another reason why the biopolymer was selected as the base.[34−36] We compared the performance of cellulose nanofilters to those coated with poly(diallyldimethyammounium chloride) (PDADMAC), a polycation, as well as with polydopamine (PDA), a bioinspired glue. Particle size fractional penetration was further analyzed to better characterize the ability to remove nanoparticles using a functionalized nanofilter. The performance of a composite filter that featured both hydrophilic cellulose and hydrophobic cellulose acetate nanofibers was also investigated in a high humidity environment. Overall, this study shows the impact of packing density and nanofilter chemistry on filter performance.

EXPERIMENTAL SECTION

Materials and Chemicals. All chemicals were used as-received. Cellulose acetate (Mw = 30000 Da by GPC, ≥97%), dopamine hydrochloride (≥98%), and a poly(diallyldimethylammonium chloride) solution (PDADMAC, 20 wt %, Mw = 200000−350000 Da) were purchased from Sigma-Aldrich (St. Louis, MO). Tris base (molecular biology), tris hydrochloride (molecular biology), acetone (histological grade), sodium hydroxide (NaOH, ACS), and ethanol (absolute anhydrous) were obtained from Fisher Scientific (Fair Lawn, NJ). Deionized (DI) water was obtained from a Barnstead Nanopure Infinity water purification system (Thermo Fisher Scientific, Waltham, MA).

Fabrication of Electrospun Cellulose Acetate and Cellulose Nanofilters. The procedure used to electrospin cellulose was based on the literature where cellulose acetate is electrospun and regenerated into cellulose nanofibers.[37] Cellulose acetate (2.25 g) was mixed with 15 mL of acetone (15% w/v) for 24 h at 20 rpm using an Arma-Rotator A-1 (Bethesda, MA) in ambient conditions. The solution was loaded into a 5 mL Luer-Lock tip syringe capped with an 18-gauge needle, which was then mounted on a PHD Ultra syringe pump (Harvard Apparatus, Plymouth, PA). A high voltage supply (Gamma High Voltage Research Inc., Ormond Beach, FL) was connected using alligator clips to the needle and a copper plate wrapped with aluminum foil. The electrospinning apparatus parameters were as follows: a constant flow rate of 3 mL/h, an applied voltage of 25 kV, and a separation distance of 10 cm. Fibers were electrospun for 30 min within an environmental chamber (CleaTech, Santa Ana, CA); a desiccant unit (Drierite, Xenia, OH) was used to maintain a temperature of 22 ± 1 °C and a relative humidity of 22%. After deposition, the cellulose acetate nanofiber filters were removed from the aluminum foil and sandwiched between Chemical-Resistant Slippery Teflon PTFE Sheets (3.2 mm × 101.6 mm × 152.4 mm, McMaster-Carr, Robbinsville, NJ). To convert the filters from cellulose acetate to cellulose, the fibers were thermally treated at 208 °C for 1 h before being submerged in a 0.1 M NaOH solution (4:1 v/v of water/ethanol) for 16 h. Next, the nanofilters were rinsed with deionized water 3 times before being placed in a desiccator overnight at room temperature. All nanofilters were punched into 2.54 cm diameter disks using a Spearhead 130 Power Punch MAXiset (Fluid Sealing Services, Wausau, WI) before further functionalization and performance evaluation.

PDA- and PDADMAC-Functionalized Nanofilters. In addition to testing cellulose nanofilters, we functionalized the filters using (i) polydopamine (PDA) and (ii) polydiallyldimethylammonium chloride (PDADMAC) based on previous literature.[38] Nanofilter samples (2.54 cm diameter disks) were placed into separate wells of a 6-well plate with 5 mL of desired functionalization solution and agitated using a shaker plate at 150 rpm for 6 h. For PDA functionalization, a Tris buffer solution (10 mM, PH 8.5) containing 2 mg/mL of dopamine hydrochloride was used. For PDADMAC functionalization, 2 mg/mL of dopamine hydrochloride and 2 mg/mL of

https://doi.org/10.1021/acs.iecr.1c03051
Ind. Eng. Chem. Res. XXXX, XXX, XXX−XXX

PDADMAC were used. After functionalization, samples were rinsed with DI water 3 times and placed onto Teflon sheets to dry overnight in a desiccator.

Characterization of Nanofilters. Scanning electron micrographs (SEM) were obtained using an FEI Magellan 400 XHR-SEM (ThermoFisher Scientific, Hillsboro, OR). Samples were sputter-coated (Cressington208 Sputter Coater, Watford, UK) with 3 nm of platinum before imaging. The fiber diameter distribution was determined by measuring 50 random fibers from 5 micrographs using *ImageJ* software.[39] A PerkinElmer Spectrum 100 Fourier transform infrared spectrometer (FTIR, Waltham, MA) was used to confirm the regeneration and functionalization of the nanofilters. High-Resolution X-ray Photoelectron Spectroscopy (XPS) scans were acquired by a Thermo Fisher Scientific Nexsa XPS to determine the chemical composition of functionalized nanofilters. The bulk thickness (Z) of each electrospun nanofilter was measured at three different locations on every electrospun sample using a Mitutoyo 293-330 digital micrometer (Toronto, Ontario, Canada).

Performance of Nanofilters to Remove Particulate Matter. Commercial mixed cellulose ester (MCE) membranes with a thickness of 150 μm were obtained from Zefon International (Ocala, FL) and used as controls. To better compare the performance of the in-house fabricated nanofilters with control filters, three nanofilters (each electrospun for 30 min) were stacked to achieve a total thickness of 150 or 330 μm. To mimic extreme hazardous air quality (PM concentration >2000 μg m^{-3}), particulate matter was generated by simultaneously burning three Hem Precious Chandan incense sticks (Hicksville, NY) in a custom-built chamber. Downstream particle concentration and particle size distribution were measured using a Model 3775 Condensation Particle Counter (CPC, TSI Incorporated, Shoreview, MN) and a Series 3080 Electrostatic Classifier (TSI Incorporated, Shoreview, MN) at a sample flow rate of 3.0 L m^{-1}, where the particle size was analyzed from 20 to 900 nm. Combined, these instruments operate together as a Scanning Mobility Particle Sizer (SMPS) and quantify the particle number based on discrete particle size ranges. The test filter was mounted on a custom-built filter module in line with a vacuum pump that had a face velocity of 15.1 cm/s using the choked flow induced by a brass critical orifice (Size 4, O'Keefe Controls Co., Trumbull, CT). The differential pressure across the filter was measured using a digital pressure gauge (SSI Technologies, LLC, Janesville, WI). All flow streams were connected using carbonized conductive tubing to reduce particle loss in the inlet. The effective area of the filter was 5 cm^2, and all filters were tested for 20 min (after allowing the particle concentration to stabilize for 10 min). Downstream particles were analyzed during the last 10 min of the test to evaluate the filter performance. Long-term filtration performance was conducted for four consecutive cycles, where the nanofilters were tested for 20 min for each cycle (80 min total). For the experiments conducted in a high humidity environment, a humidifier was placed in the chamber to increase the relative humidity to 80%.

RESULTS AND DISCUSSION

Chemical Characteristics of Cellulose and Functionalized Nanofilters. Cellulose nanofilters were successfully fabricated using electrospinning, and to explore the role of chemistry on filter performance, we also performed two surface chemical modifications. First, to manufacture the base material, we electrospun cellulose acetate nanofilters and using an alkaline treatment regenerated them into pure cellulose.[37] The FTIR spectra of the as-spun cellulose acetate and regenerated cellulose are provided in Figure 1. The disappearance of the

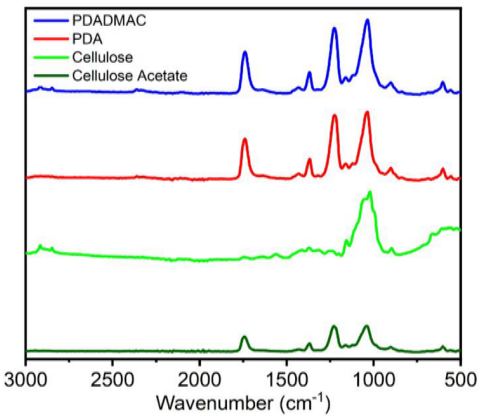

Figure 1. FTIR spectra for as-spun cellulose acetate and regenerated cellulose nanofilters, as well as the PDA- and PDADMAC-functionalized nanofilters.

1750 cm^{-1} peak in the cellulose nanofilter spectra after the alkaline treatment indicates that the acetate groups have been replaced with hydroxyl groups, supporting the successful regeneration from cellulose acetate.

A representative SEM micrograph of the cellulose nanofilters is provided in Figure 2(a). While an in-depth comparison of

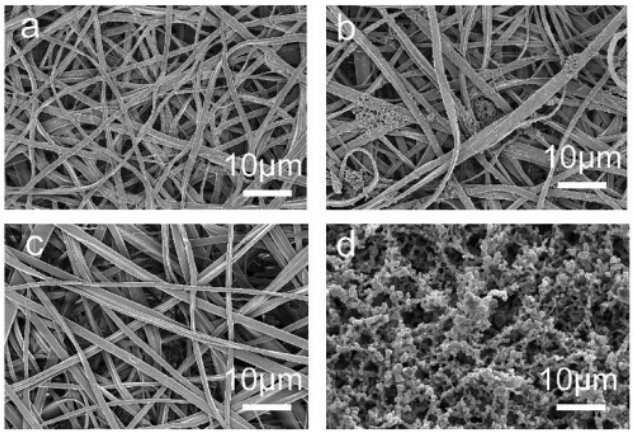

Figure 2. Scanning electron micrographs of (a) cellulose, (b) PDA-functionalized, and (c) PDADMAC-functionalized nanofilters. (d) Micrograph of the commercial mixed cellulose ester (MCE) filter that served as a control material in the filtration experiments.

the fiber morphology and its relevance for air purification will be provided in the section Morphological Characteristics of Cellulose and Functionalized Nanofilters, it is important to note that the cellulose acetate and cellulose nanofilters were easily electrospun into freestanding meshes that could be handled and used in filtration tests or as a base material for further chemical functionalizations. The Experimental Section details the procedure used to functionalize the cellulose nanofilters with the bioinspired glue, polydopamine (PDA), or with cationic charges using poly(diallyldimethyammounium chloride) (PDADMAC). Throughout the rest of the Results

https://doi.org/10.1021/acs.iecr.1c03051
Ind. Eng. Chem. Res. XXXX, XXX, XXX−XXX

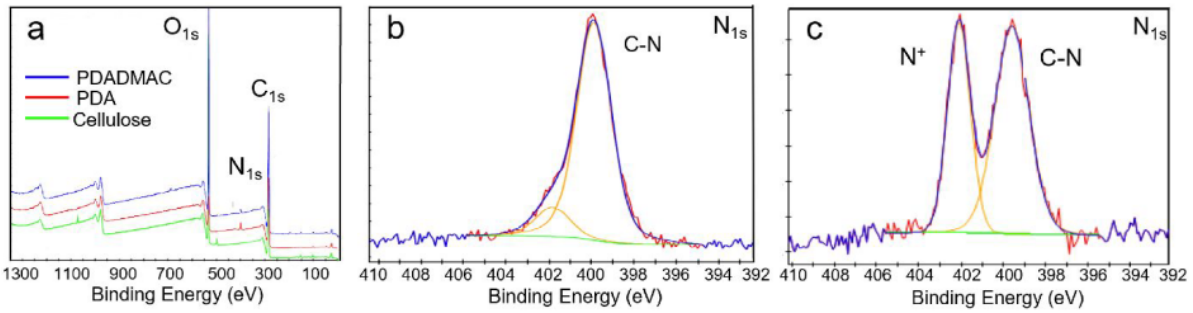

Figure 3. XPS spectra of (a) survey scans including cellulose, PDA, and PDADMAC nanofilters and a high-resolution scan of N_{1s} for (b) PDA and (c) PDADMAC nanofilters as a function of binding energy (eV).

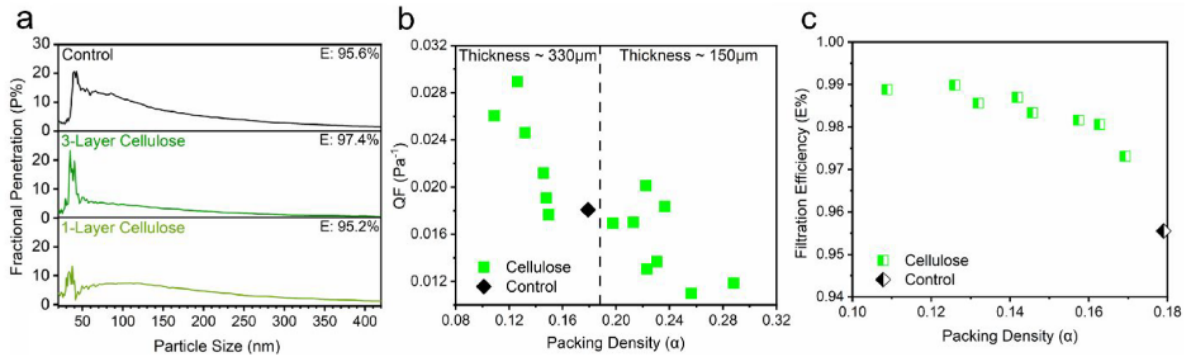

Figure 4. (a) Fractional penetration as a function of the particle electrical mobility diameter ranging from 20 to 400 nm for a single layer cellulose nanofilter, multilayer cellulose nanofilter, and commercial MCE control. The overall filtration efficiency (E) is also displayed. (b) Quality factor (QF) as a function of packing density for the cellulose nanofilters and MCE controls. The dotted line separates the filters that had a total bulk thickness of 330 μm from those that were 150 μm thick. (c) Filtration efficiency (E) as a function of packing density for the cellulose nanofilters and MCE controls. All samples had a total filter thickness of 330 μm.

and Discussion section, we will refer to these samples as PDA and PDADMAC nanofilters, respectively.

FTIR peaks displayed in the spectra of PDA and PDADMAC nanofibers around 1250 and 1500 cm^{-1} indicate the presence of aromatic rings from the deposition of polydopamine.[40,41] To further confirm the successful coating of PDA and PDADMAC on cellulose nanofilters, elemental data analysis via representative survey scans and high resolution XPS for carbon, oxygen, and nitrogen were obtained, see Figure 3. The elemental analysis data is also summarized in Table S1. XPS narrow-scan analysis of the N_{1s} showed a signal at 399 eV for both functionalized nanofilters that was not present on the bare cellulose nanofilter, which confirms the presence of polydopamine, since the 399 eV signal was due to the primary amine group.[42] Another N_{1s} signal around 402 eV is displayed in Figure 3(c) and indicates the presence of the positively charged nitrogen atoms on PDADMAC, which distinguishes the two functionalized samples we synthesized.[40]

Morphological Characteristics of Cellulose and Functionalized Nanofilters. Scanning electron microscopy (SEM) was utilized to analyze the morphology and the fiber diameter distribution of the nanofilters, as displayed in Figures 2(a–c) and S1. The micrographs show that all filters exhibit randomly accumulated and continuous fibers; no fiber ends are displayed. Also, the micrograph suggests that the fibers are interconnected and that the pores between the fibers are much larger than the diameter of the nanofibers. The cellulose nanofilters in Figure 2(a) had a smooth and cylindrical morphology with an average fiber diameter of 0.9 ± 0.3 μm, consistent with our previous report.[43] When functionalized with PDA, the surface of the nanofilters was decorated with small particles aggregated throughout the fibers, thus giving a larger fiber diameter at 1.4 ± 0.4 μm. The PDADMAC nanofilters exhibited a smooth morphology and the largest average fiber diameter of 1.7 ± 0.7 μm. Based on previous studies,[38,44] we estimate that the pore size and specific surface area of all the in-house fabricated nanofilters are 4–8 μm and 4.5 m^2/g, respectively, which strongly suggests that the nanofilters do not remove particles by trapping or sieving since the size of the incense particles investigated is in the submicron and nanoscale range.

A representative SEM micrograph of the commercial MCE control filter is shown in Figure 2(d), which displays their lace-like structure.[45] The manufacturer reports that the MCE filters are one of the most widely used filters in both air monitoring and analytical applications and that they are produced from a mixture of cellulose acetate and cellulose nitrate with a porosity of 82% and a pore size of 0.8 μm.[46] Next, we explored if the greater interconnectivity of electrospun nanofibers could effectively capture more particles than the commercial MCE control filters.

Nanofilter Layering and Overall Filtration Performance. Our first goal was to determine the optimal thickness of our in-house electrospun filters using the base cellulose nanofilters. Using the same electrospinning apparatus conditions, but different time durations, we produced consistent morphology nanofibers with different total bulk thicknesses of 50 or 110 μm, which were used either as an individual layer or as a multilayered filter. Figures 4(a) and S2 provide a

https://doi.org/10.1021/acs.iecr.1c03051
Ind. Eng. Chem. Res. XXXX, XXX, XXX−XXX

schematic as well as summarize the packing density (α) of all the cellulose nanofilters investigated in this work, as calculated using eq 2. Given the nonuniform nature of the electrospinning process (i.e., fibers randomly accumulate on the collector plate), the packing density of the filters varied despite the overall bulk thickness being equivalent. Notably, the packing density of all ~150 μm thick cellulose nanofilters was higher than that of the commercial control, whereas the packing density of the thicker filters tended to be lower than the control.

The performance of 110 μm thick single-layered nanofilters was compared to the 330 μm thick layered filters, and the particle fractional penetration is shown in Figure 4(a). Notably, the multilayer cellulose filters showed higher removal efficiency (E: 97.4%) and displayed a greater particle selectivity for particles over 50 nm in diameter than single layer and even control filters. The benefit of stacking multiple filters was consistent with previous work,[27] which showed that there was an improvement in filtration efficiency without altering the quality factor (QF). The relationship between packing density and quality factor is shown in Figures 4(b) and S3; filters with a greater thickness and lower packing density exhibited a higher quality factor, meaning a greater overall filter performance. Therefore, 3-layer nanofilters with a total thickness of ~330 μm were investigated throughout the remainder of this work. Notably, the filtration efficiency of the cellulose nanofilters was found to have a negative trend associated with packing density, as displayed in Figure 4(c), whereas increases in packing density were associated with a decrease in filtration efficiency. In recent reports, filtration efficiency was found to be greater for thicker mats; however, there was no clear correlation between packing density and filtration efficiency.[27−29] A possible explanation for our observed trend is that less packed filters exhibit a greater effective surface area available for particle capture by diffusion and interception.[14]

Nanofilter Packing Density and Air Filtration Performance. The relationship between packing density versus filtration efficiency and pressure drop is summarized in Figures 5 and S4, for multilayered filters that had a bulk thickness of 330 μm. PDA- and PDADMAC-functionalized nanofilters were also investigated where slight decreases in filtration efficiency were observed for PDADMAC-functionalized nanofilters compared to cellulose samples with similar packing density. Due to the challenges of electrospinning filters with precisely the same packing density, these plots are meant to display the spread of data, instead of collapsing the data into an average with error bars. No obvious trend was observed for PDA-functionalized nanofilters. Since the average fiber diameter increased after functionalization for PDA and PDADMAC, the filtration efficiency was expected to decrease based on previous studies.[26,29,35,47] Notably, the surface roughness of PDA fibers and positively charged PDADMAC nanofilters can also improve the filtration performance either by an enhancement of the surface-to-volume ratio or additional electrostatic interactions.[24,48,49]

On the other hand, a pressure drop was found to have a slight positive trend associated with the packing density for the PDA- and PDADMAC-functionalized nanofilters, where no trend was observed for the cellulose nanofilters. Additionally, most of our thicker filters outperformed the commercial control filters, in terms of their quality factor. Most importantly, all nanofilters showed a much lower pressure drop compared to the typical range for traditional commercial

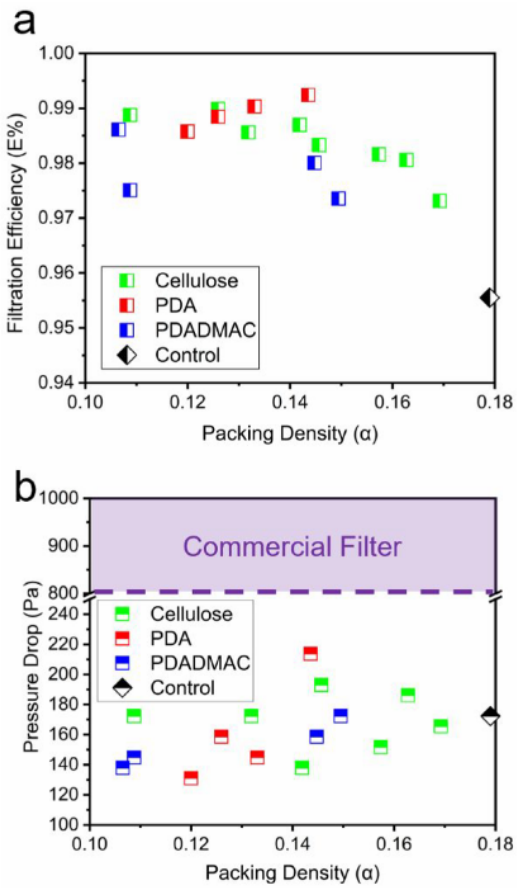

Figure 5. (a) Filtration efficiency (E) and (b) pressure drop as a function of packing density for MCE control, cellulose, PDA, and PDADMAC nanofilters. All samples had a total filter thickness of 330 μm.

filters, as noted by the horizontal purple highlighted area in Figure 5(b); these commercial filters have been reported to have a 99.58% removal efficiency.[10,18,24] Srikrishnarka et al. reported that chemically treated electrospun fibers with increased surface charge, either negative or positive, showed improved filtration efficiency for a particle size smaller than 300 nm.[48] These data suggest that greater filter performance can be achieved by electrospinning a filter with a lower packing density. We next investigate the effect that additional functional groups introduced by PDA and PDADMAC functionalization have on particle fractional penetration.

Selectivity and Particle Fractional Penetration of Nanofilters. According to classical filtration theory, there are five capture mechanisms, Brownian diffusion, electrostatic interaction, interception, inertial impaction, and gravity settling, based on the fluid dynamics of a particle with the air stream and the ratio of various forces acting on the particles, which will dominate in different particle size ranges.[10,11,50−52] Brownian motion and electrostatic interaction are significant as the particle size decreases (<0.1 μm), which make them the primary capture mechanisms for nanoscale particles. If particles on the order of 0.3−1.0 μm follow the streamline well, they will only intercept the fibers within the filter if they are within one particle radius from a fiber. For particles larger than 1.0 and 10 μm, inertial impaction and gravity settling dominate, respectively. We have provided this breakdown of removal mechanisms to clarify that there is no single capture

https://doi.org/10.1021/acs.iecr.1c03051
Ind. Eng. Chem. Res. XXXX, XXX, XXX−XXX

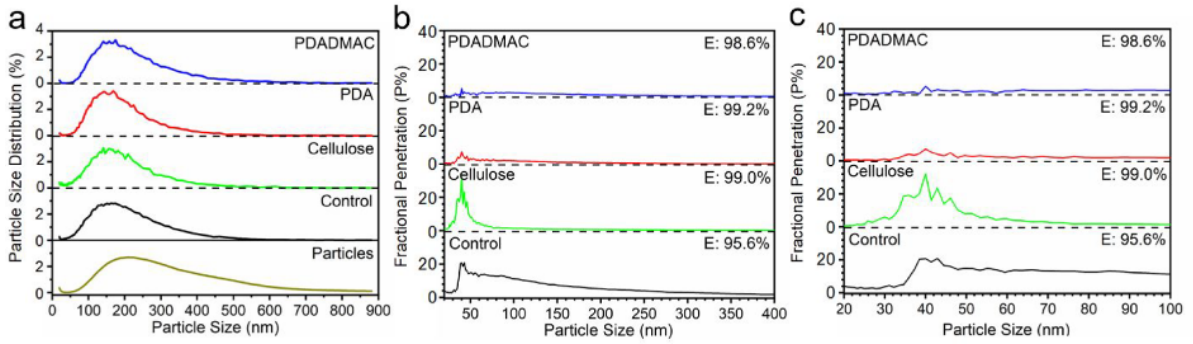

Figure 6. (a) Normalized particle size distribution for incense particles (upstream) and downstream particles for MCE control, cellulose, PDA, and PDADMAC nanofilters. Fractional penetration as a function of particle electrical mobility diameter ranging from (b) 20 to 400 nm and (c) 20 to 100 nm for MCE control, cellulose, PDA, and PDADMAC nanofilters. Overall filtration efficiency (E) is displayed in the upper right-hand corner.

Table 1. Summary of the Nanofilter Properties and Air Filtration Performance for Samples Exhibiting over 97.0% Overall Filtration Efficiency

filter	fiber diameter (μm)	E^a (%)	ΔP (Pa)	QF (Pa^{-1})	MPPS (nm)	P^b (%)
cellulose	0.9 ± 0.3	98.4 ± 0.5	167 ± 17.9	0.025 ± 0.003	142.1 ± 7.5	21.2 ± 5.1
PDA	1.4 ± 0.4	98.9 ± 0.3	162 ± 36.3	0.029 ± 0.004	147.5 ± 10.3	13.4 ± 5.5
PDADMAC	1.7 ± 0.7	97.9 ± 0.5	153 ± 15.3	0.027 ± 0.004	164.2 ± 8.8	3.95 ± 1.52
MCE control	NA	95.7 ± 0.9	190 ± 17.3	0.017 ± 0.001	153.3 ± 11.3	16.7 ± 0.87

[a]Particulates ranging from 20 to 900 nm were studied in this work. [b]Penetration of 41.4 nm particles.

mechanism that dominates for 0.1−0.3 μm diameter particles and to note that this size range is where commercial filters usually demonstrate the lowest overall collection efficiency, i.e., the most penetrating particle size (MPPS).[10,27] Normally, the MPPS is about 0.3 μm for air filters, and its corresponding filtration efficiency is used to classify air filters.[10,11] For instance, a High-Efficiency Particulate (HEPA) filter captures at least 99.97% of particles as small as 0.3 μm.

To further investigate the particle size selectivity of all filters, we tested the ability to remove downstream particles with diameters ranging from 20 to 900 nm using a scanning mobility particle sizer (SMPS). Figure 6(a) shows the normalized distribution of the upstream aerosolized particles and downstream particles collected by the SMPS. Notice that only nanofilters with over 97.0% overall filtration efficiency are displayed in Figure 6 and Table 1. The MPPS for control, cellulose, PDA, and PDADMAC nanofilters was 162.5, 140.7, 168.5, and 174.7 nm, respectively. As stated in the literature,[27,53] MPPS decreases with a decreasing fiber diameter, which corresponds with our results, since the average fiber diameter for cellulose, PDA, and PDADMAC was 0.9, 1.4, and 1.7 μm, respectively. As a note, determining the average fibril diameter for the commercial controls was not possible due to their lace-like structure, see Figure 2(d).

The fractional penetration for different particle sizes was calculated by determining the ratio of particles downstream to those upstream of the filter, as displayed in Figure 6(b and c). The overall filtration efficiency for each sample is displayed in the upper right-hand corner of the figure, and the fractional penetration is plotted in the range of 0−40%. Only particles smaller than 400 nm are shown in Figure 6(b), since at least 98% fractional removal was achieved for particle sizes larger than 400 nm for cellulose, PDA, and PDADMAC nanofilters. Based on our results, we note that the nanofilters demonstrated an outstanding ability to remove particles larger than 70 nm compared to the control filter. Given that the nanofilter and control filter have a similar chemical composition, we hypothesize that the fiber interconnectivity of the nanofilter leads to the better capture of particles by interception than the commercial control. From Figure 6(c), particles around 42 nm showed the highest fractional penetration at 19.0, 34.7, 5.26 and 2.32% for control, cellulose, PDA, and PDADMAC, respectively. Since nanoparticle capture is mainly dominated by diffusion and electrostatic interactions, the (nonstatistical) difference in the fiber diameter likely had only a subtle effect. The additional functional groups from PDA (i.e., thiols and amines[54]) and positively charged surfaces from the PDADMAC coatings greatly improved the capture of particles from 30 to 60 nm compared to the bare cellulose nanofilters. The physical properties and air filtration performance metrics of all the filters analyzed are summarized in Table 1. Overall, the PDADMAC nanofilters demonstrated the best particle penetration resistance for all particle sizes among all samples.

Long-Term Filtration Performance. The long-term performance of the cellulose nanofilters was also investigated by conducting four consecutive filtration efficiency experiments. After the four cycles, the pressure drop increased by just 5%, and a slight increase in filtration efficiency was observed. The particle fractional penetration for each cycle is displayed in Figure 7(a). The highest particle fractional penetration percent and filtration efficiency for each cycle were determined to be 27.9, 12.5, 43.1, 17.9% and 97.0, 99.0, 99.0, 98.2%, respectively. Filtration efficiency and pressure drop are both expected to increase, since the pores will be obstructed by particles.[16,24] The fluctuation of fractional penetration for particles smaller than 50 nm likely resulted due to different electrostatic interactions that resulted once the incense particles were deposited on the filters. Notably, the filters remained intact even after being used in multiple filtration tests. SEM images of the cellulose nanofilters after the first and fourth cycles are displayed in Figure 7(b and c), respectively. As one would expect, there are more particles observed and deposited on the fibers after the fourth filtration cycle, but the pores remain available (i.e., not clogged). Additionally, the

https://doi.org/10.1021/acs.iecr.1c03051
Ind. Eng. Chem. Res. XXXX, XXX, XXX−XXX

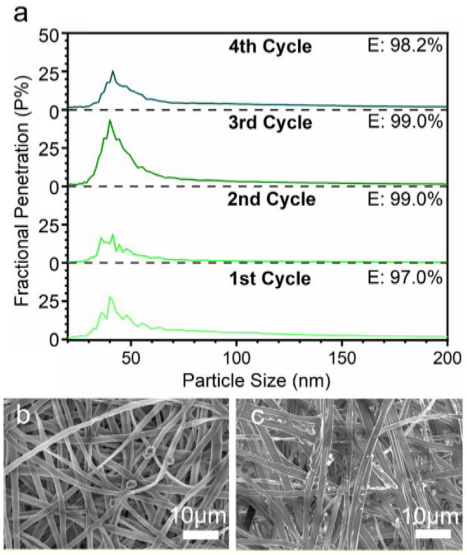

Figure 7. (a) Particle fractional penetration percent and filtration efficiency (E) of cellulose nanofilters for each cycle of filtration. SEM micrographs of cellulose nanofilters after (b) one and (c) four cycles. After four filtration cycles, the pressure drop increased by less than 5%.

SEM images only displayed continuous fibers: even after being used in testing conditions, no broken nanofibers were observed. In conclusion, the in-house fabricated cellulose nanofilters still perform effectively after 80 min of usage in extremely high particle concentration environments. We have provided a comparison of our nanofilter's filtration properties to recent studies, which is shown in Table 2.

High Humidity Cellulose Nanofilter Performance. When moisture obstructs the pores within a filter, both the filtration efficiency is reduced due to the dissipation of the charges on the fibers and, also, the thermal-physiological comfort is decreased, which is important if the filters are to be utilized in personal protection masks. To improve the applicability of the filters in a high humidity environment, Zhao et al.[55] proposed a composite superhydrophilic/hydrophobic gradient structure that increases the moisture-vapor transmission rate (MVTR), which also offered an easy-to-clean property. Hydrophilic nanofibers exhibit high water adsorption and diffusion rate but tend to form capillary water films that increase air resistance dramatically over time under high humidity. On the other hand, hydrophobic nanofibers have low MVTR and, thus, result in poor thermal-physiological comfort. To incorporate the two distinct wetting properties, superhydrophilic polyacrylonitrile/silicon dioxide fibers and hydrophobic polyvinylidene fluoride fibers were layered to enhance the driving force of the moisture transmission rate and, at the same time, prevent a capillary water film from filming.

Inspired by this report, we fabricated a gradient filter structure using hydrophilic cellulose and hydrophobic cellulose acetate nanofilters. Contact angle measurement shown in Figure 8(a) displays that a water drop was immediately adsorbed on the cellulose nanofilters, which indicates its total-wetting property, where cellulose acetate exhibited a non-wetting property with a contact angle of 145°. A layer of a hydrophobic cellulose acetate filter was stacked under two layers of cellulose filters to form a composite filter; the schematic of the filters is displayed in Figure 8(b).

We tested the performance of our cellulose/cellulose acetate (hydrophilic/hydrophobic) composite filters in an 80% relative humidity environment, and the results are shown in Figure 8(c). In this experiment, a large number of particles penetrated the cellulose nanofilters along with water droplets, where we observed a 78.8% filtration efficiency and a pressure drop of 27.6 Pa under these conditions. These data suggest that the capillary film makes the hydrophilic filter much more penetrable for both particles and water droplets while at the same time decreasing the air resistance of the filter. By introducing the composite structure, the filtration efficiency dramatically increased to 99.8% with a pressure drop of 158 Pa, which means the filter performance was comparable to filtration conducted in a low humidity environment. SEM micrographs of the cellulose nanofilters after testing in a high humidity environment are displayed in Figure 8(d), where the fiber morphology remains unchanged and particles were again observed as being trapped within the filter. The composite filter demonstrated a superior removal of particles across the size from 20 to 900 nm in comparison to the cellulose and control filters. Furthermore, after the first testing cycle conducted on the commercial control filter, a 27% increase in the pressure drop was observed, whereas the composite filter remained unchanged.

CONCLUSIONS

Surface functionalized nanofilters demonstrated improved filtration efficiency for removing nanoscale particulate matter compared to untreated and commercial control filters. The

Table 2. Comparison of Nanofilter Properties and Air Filtration Performance from Recent Studies[a]

filter chemistry	surface modification/other characteristic	fiber diameter (μm)	E (%)	ΔP (Pa)	QF (Pa^{-1})	stability	ref
cellulose		0.9	98.4[d]	167	0.025	99.8% (E) at 80% RH	this work
cellulose	PDA-functionalized	1.4	98.9[d]	162	0.029		this work
cellulose	PDADMAC-functionalized	1.7	97.9[d]	153	0.027		this work
PI	R-TENG enhanced	≅0.2	>97[d]	180	>0.019		30
PAN	oxygen plasma	≅0.3	94.02[c]	18	0.16	1% (E), 1 Pa (ΔP) decrease after 50 cycles	24
PS, PAN	chemically charged	0.45	99.01[d]	<60	>0.077	99.92% (E) after 24 h	48
PVDF	fiber/net 2D networks	0.021	99.99[b]	93	0.11	no change in E%, 6 Pa (ΔP) increase after 100 h	31
TPU	nanofiber/net	<0.05	97.08[d]	58	0.061	10% (E%) decrease after 24 h	32

[a]Filter chemistry abbreviations: PI: polyimide, PAN: polyacrylonitrile, PS: polystyrene, PVDF: polyvinylidene fluoride, TPU: thermoplastic polyurethane, R-TENG: rotating triboelectric nanogenerator. [b]E (%) was measured for $PM_{0.3}$. [c]E (%) was measured for $PM_{2.5}$. [d]E (%) was measured for $PM_{0.9}$.

https://doi.org/10.1021/acs.iecr.1c03051
Ind. Eng. Chem. Res. XXXX, XXX, XXX−XXX

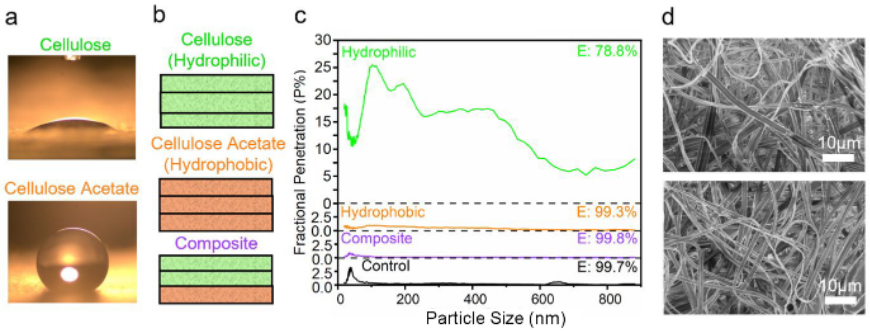

Figure 8. (a) Contact angle measurement for cellulose and cellulose acetate nanofilters. (b) Schematic diagram of cellulose, cellulose acetate, and composite gradient filter structure. (c) Fractional penetration as a function of particle size ranging from 20 to 900 nm. (d) SEM micrographs of cellulose nanofilters after one cycle of high humidity filtration.

improvement in filtration performance was due to the presence of additional electrostatic interactions provided by the cationic polymer, PDADMAC, and the bioinspired glue, PDA. Optimal thickness of the nanofilters was determined by the packing density and its corresponding overall filtration performance (i.e., quality factor). Under extremely polluted sampling conditions, untreated cellulose nanofilters and PDA- and PDADMAC-functionalized nanofilters maintained a filtration efficiency of 99.0%, 99.2%, and 98.6%, respectively, in removing incense particles in the size range from 20 to 900 nm. This represents a substantial improvement in filtration efficiency for each of our tested nanofibers over the commercially available mixed cellulose ester control filters. PDA- and PDADMAC-functionalized nanofilters greatly improved the removal of the highest fractional penetration particles, from 34.7% to 5.26% and 2.32%, respectively, whereas PDADMAC showed the lowest pressure drop (138 Pa) and highest quality factors (0.031 Pa^{-1}). When long-term, multicycle filtration tests were conducted using the cellulose nanofilters, only a 5% increase in the pressure drop was observed after 80 min of continuous filtration. By introducing a cellulose (hydrophilic) and cellulose acetate (hydrophobic) composite structure, we were able to achieve a 99.8% filtration efficiency in an 80% relative humidity environment. We suggest that the nanofilters used in this study can efficiently remove nanoscale particulate matter, even when used in a high humidity environment.

■ ASSOCIATED CONTENT

Supporting Information

The Supporting Information is available free of charge at https://pubs.acs.org/doi/10.1021/acs.iecr.1c03051.

Fiber diameter distributions, XPS data, plots of packing density versus bulk nanofiber thickness, filtration efficiency, pressure drop, and quality factor (PDF)

■ AUTHOR INFORMATION

Corresponding Author

Jessica D. Schiffman − *Department of Chemical Engineering, University of Massachusetts Amherst, Amherst, Massachusetts 01003-9303, United States;* orcid.org/0000-0002-1265-5392; Phone: (413) 545-6143; Email: schiffman@ecs.umass.edu

Authors

Shao-Hsiang Hung − *Department of Chemical Engineering, University of Massachusetts Amherst, Amherst, Massachusetts 01003-9303, United States;* orcid.org/0000-0001-8160-2668

Jared W. Bowden − *Department of Chemical Engineering, University of Massachusetts Amherst, Amherst, Massachusetts 01003-9303, United States*

Richard E. Peltier − *School of Public Health & Health Sciences, University of Massachusetts Amherst, Amherst, Massachusetts 01003-9303, United States*

Complete contact information is available at: https://pubs.acs.org/10.1021/acs.iecr.1c03051

Notes

The authors declare no competing financial interest.

Biographies

Shao-Hsiang Hung is currently a Ph.D. student in Chemical Engineering at the University of Massachusetts Amherst. He holds B.S. and M.S. degrees in Chemical Engineering from the National Taiwan University and the University of Massachusetts Amherst, respectively. His research experiences include investigating the environmental applications of electrospun cellulose nanofilters and metal−organic framework (MOF) membranes for applications, such as particulate matter removal and organic solvent pervaporation. His ongoing research focuses on fabricating next-generation phase inversion water purification membranes using polyelectrolytes, which aims to eliminate the use of harmful organic solvents during the membrane synthesis process.

https://doi.org/10.1021/acs.iecr.1c03051
Ind. Eng. Chem. Res. XXXX, XXX, XXX−XXX

Jessica D. Schiffman is an Associate Professor and the Interim Department Head of Chemical Engineering at the University of Massachusetts Amherst. She holds B.S., M.Eng., and Ph.D. degrees in Materials Science and Engineering from Rutgers University, Cornell University, and Drexel University, respectively. Afterward, she completed postdoctoral training in Environmental Engineering at Yale University. Professor Schiffman directs an interdisciplinary and imaginative research group that innovates polymer-based materials that address grand challenges in human health and the environment. She has recently been named a 2021 Influential Researchers by *I&EC Research*, and in 2019, she was awarded the *ACS Applied Materials & Interfaces* Young Investigator Award. From UMass Amherst, she was awarded the College of Engineering Outstanding Teaching Award, as well as the College of Engineering Barbara & Joseph Goldstein Outstanding Junior Faculty Award.

■ ACKNOWLEDGMENTS

We thank Paul Mack at Thermo Fisher Scientific for assistance with XPS experiments. J.W.B. thanks the Commonwealth Honors College for support. The authors acknowledge the support of the National Science Foundation (NSF), award number 2029371.

■ REFERENCES

(1) World Health Organization. *World health statistics 2018: monitoring health for the SDGs, sustainable development goals*; World Health Organization: 2018.

(2) World Health Organization. *Ambient air pollution: a global assessment of exposure and burden of disease*; World Health Organization: 2016.

(3) Konda, A.; Prakash, A.; Moss, G. A.; Schmoldt, M.; Grant, G. D.; Guha, S. Aerosol Filtration Efficiency of Common Fabrics Used in Respiratory Cloth Masks. *ACS Nano* **2020**, *14* (5), 6339−6347.

(4) Armentano, I.; Barbanera, M.; Carota, E.; Crognale, S.; Marconi, M.; Rossi, S.; Rubino, G.; Scungio, M.; Taborri, J.; Calabrò, G. Polymer Materials for Respiratory Protection: Processing, End Use, and Testing Methods. *ACS Applied Polymer Materials* **2021**, *3* (2), 531−548.

(5) Shen, H.; Zhou, Z.; Wang, H.; Zhang, M.; Han, M.; Durkin, D. P.; Shuai, D.; Shen, Y. Development of Electrospun Nanofibrous Filters for Controlling Coronavirus Aerosols. *Environ. Sci. Technol. Lett.* **2021**, *8* (7), 545−550.

(6) Mannucci, P. M.; Harari, S.; Martinelli, I.; Franchini, M. Effects on health of air pollution: a narrative review. *Internal and Emergency Medicine* **2015**, *10* (6), 657−662.

(7) Mentz, R. J.; Roessig, L.; Greenberg, B. H.; Sato, N.; Shinagawa, K.; Yeo, D.; Kwok, B. W. K.; Reyes, E. B.; Krum, H.; Pieske, B.; Greene, S. J.; Ambrosy, A. P.; Kelly, J. P.; Zannad, F.; Pitt, B.; Lam, C. S. P. Heart Failure Clinical Trials in East and Southeast Asia. *JACC: Heart Failure* **2016**, *4* (6), 419−427.

(8) Timonen, K. L.; Vanninen, E.; De Hartog, J.; Ibald-Mulli, A.; Brunekreef, B.; Gold, D. R.; Heinrich, J.; Hoek, G.; Lanki, T.; Peters, A.; Tarkiainen, T.; Tiittanen, P.; Kreyling, W.; Pekkanen, J. Effects of ultrafine and fine particulate and gaseous air pollution on cardiac autonomic control in subjects with coronary artery disease: The ULTRA study. *J. Exposure Sci. Environ. Epidemiol.* **2006**, *16* (4), 332−341.

(9) Philip, S.; Martin, R. V.; Van Donkelaar, A.; Lo, J. W.-H.; Wang, Y.; Chen, D.; Zhang, L.; Kasibhatla, P. S.; Wang, S.; Zhang, Q.; Lu, Z.; Streets, D. G.; Bittman, S.; Macdonald, D. J. Global Chemical Composition of Ambient Fine Particulate Matter for Exposure Assessment. *Environ. Sci. Technol.* **2014**, *48* (22), 13060−13068.

(10) Zhu, M.; Han, J.; Wang, F.; Shao, W.; Xiong, R.; Zhang, Q.; Pan, H.; Yang, Y.; Samal, S. K.; Zhang, F.; Huang, C. Electrospun Nanofibers Membranes for Effective Air Filtration. *Macromol. Mater. Eng.* **2017**, *302* (1), 1600353.

(11) Li, P.; Wang, C.; Zhang, Y.; Wei, F. Air Filtration in the Free Molecular Flow Regime: A Review of High-Efficiency Particulate Air Filters Based on Carbon Nanotubes. *Small* **2014**, *10* (22), 4543−4561.

(12) Ahmed, F. E.; Lalia, B. S.; Hashaikeh, R. A review on electrospinning for membrane fabrication: Challenges and applications. *Desalination* **2015**, *356*, 15−30.

(13) Schiffman, J. D.; Schauer, C. L. A Review: Electrospinning of Biopolymer Nanofibers and their Applications. *Polym. Rev.* **2008**, *48* (2), 317−352.

(14) Wang, Z.; Zhao, C.; Pan, Z. Porous bead-on-string poly(lactic acid) fibrous membranes for air filtration. *J. Colloid Interface Sci.* **2015**, *441*, 121−9.

(15) Bortolassi, A. C. C.; Nagarajan, S.; de Araujo Lima, B.; Guerra, V. G.; Aguiar, M. L.; Huon, V.; Soussan, L.; Cornu, D.; Miele, P.; Bechelany, M. Efficient nanoparticles removal and bactericidal action of electrospun nanofibers membranes for air filtration. *Mater. Sci. Eng., C* **2019**, *102*, 718−729.

(16) Lee, S.; Cho, A. R.; Park, D.; Kim, J. K.; Han, K. S.; Yoon, I.-J.; Lee, M. H.; Nah, J. Reusable Polybenzimidazole Nanofiber Membrane Filter for Highly Breathable PM2.5 Dust Proof Mask. *ACS Appl. Mater. Interfaces* **2019**, *11* (3), 2750−2757.

(17) Matulevicius, J.; Kliucininkas, L.; Prasauskas, T.; Buivydiene, D.; Martuzevicius, D. The comparative study of aerosol filtration by electrospun polyamide, polyvinyl acetate, polyacrylonitrile and cellulose acetate nanofiber media. *J. Aerosol Sci.* **2016**, *92*, 27−37.

(18) Liu, C.; Hsu, P.-C.; Lee, H.-W.; Ye, M.; Zheng, G.; Liu, N.; Li, W.; Cui, Y. Transparent air filter for high-efficiency PM2.5 capture. *Nat. Commun.* **2015**, *6* (1), 6205.

(19) Xu, J.; Liu, C.; Hsu, P.-C.; Liu, K.; Zhang, R.; Liu, Y.; Cui, Y. Roll-to-Roll Transfer of Electrospun Nanofiber Film for High-Efficiency Transparent Air Filter. *Nano Lett.* **2016**, *16* (2), 1270−1275.

(20) Wang, C.; Wu, S.; Jian, M.; Xie, J.; Xu, L.; Yang, X.; Zheng, Q.; Zhang, Y. Silk nanofibers as high efficient and lightweight air filter. *Nano Res.* **2016**, *9* (9), 2590−2597.

(21) Zhang, R.; Liu, C.; Hsu, P.-C.; Zhang, C.; Liu, N.; Zhang, J.; Lee, H. R.; Lu, Y.; Qiu, Y.; Chu, S.; Cui, Y. Nanofiber Air Filters with High-Temperature Stability for Efficient PM2.5 Removal from the Pollution Sources. *Nano Lett.* **2016**, *16* (6), 3642−3649.

(22) Wei, Z.; Su, Q.; Wang, X.; Long, S.; Zhang, G.; Lin, Q.; Yang, J. Nanofiber Air Filters with High-Temperature Stability and Superior Chemical Resistance for the High-Efficiency PM2.5 Removal. *Ind. Eng. Chem. Res.* **2021**, *60* (27), 9971−9982.

(23) Cui, J.; Lu, T.; Li, F.; Wang, Y.; Lei, J.; Ma, W.; Zou, Y.; Huang, C. Flexible and transparent composite nanofibre membrane that was fabricated via a "green" electrospinning method for efficient particulate matter 2.5 capture. *J. Colloid Interface Sci.* **2021**, *582*, 506−514.

(24) Kim, H.-J.; Park, S. J.; Park, C. S.; Le, T.-H.; Hun Lee, S.; Ha, T. H.; Kim, H.-i.; Kim, J.; Lee, C.-S.; Yoon, H.; Kwon, O. S. Surface-modified polymer nanofiber membrane for high-efficiency microdust capturing. *Chem. Eng. J.* **2018**, *339*, 204−213.

https://doi.org/10.1021/acs.iecr.1c03051
Ind. Eng. Chem. Res. XXXX, XXX, XXX−XXX

(25) Yun, K. M.; Suryamas, A. B.; Iskandar, F.; Bao, L.; Niinuma, H.; Okuyama, K. Morphology optimization of polymer nanofiber for applications in aerosol particle filtration. *Sep. Purif. Technol.* **2010**, *75* (3), 340−345.
(26) Balgis, R.; Kartikowati, C. W.; Ogi, T.; Gradon, L.; Bao, L.; Seki, K.; Okuyama, K. Synthesis and evaluation of straight and bead-free nanofibers for improved aerosol filtration. *Chem. Eng. Sci.* **2015**, *137*, 947−954.
(27) Leung, W. W.-F.; Hung, C.-H.; Yuen, P.-T. Effect of face velocity, nanofiber packing density and thickness on filtration performance of filters with nanofibers coated on a substrate. *Sep. Purif. Technol.* **2010**, *71* (1), 30−37.
(28) Hung, C.-H.; Leung, W. W.-F. Filtration of nano-aerosol using nanofiber filter under low Peclet number and transitional flow regime. *Sep. Purif. Technol.* **2011**, *79* (1), 34−42.
(29) Bian, Y.; Wang, S.; Zhang, L.; Chen, C. Influence of fiber diameter, filter thickness, and packing density on PM2.5 removal efficiency of electrospun nanofiber air filters for indoor applications. *Building and Environment* **2020**, *170*, 106628.
(30) Gu, G. Q.; Han, C. B.; Lu, C. X.; He, C.; Jiang, T.; Gao, Z. L.; Li, C. J.; Wang, Z. L. Triboelectric Nanogenerator Enhanced Nanofiber Air Filters for Efficient Particulate Matter Removal. *ACS Nano* **2017**, *11* (6), 6211−6217.
(31) Liu, H.; Zhang, S.; Liu, L.; Yu, J.; Ding, B. High-Performance PM0.3 Air Filters Using Self-Polarized Electret Nanofiber/Nets. *Adv. Funct. Mater.* **2020**, *30* (13), 1909554.
(32) Chen, R.; Zhang, H.; Wang, M.; Zhang, X.; Gan, Z. Thermoplastic Polyurethane Nanofiber Membrane Based Air Filters for Efficient Removal of Ultrafine Particulate Matter PM0.1. *ACS Applied Nano Materials* **2021**, *4* (1), 182−189.
(33) Dobosz, K. M.; Kolewe, K. W.; Schiffman, J. D. Green materials science and engineering reduces biofouling: approaches for medical and membrane-based technologies. *Front. Microbiol.* **2015**, *6*, 196.
(34) Frey, M. W. Electrospinning Cellulose and Cellulose Derivatives. *Polym. Rev.* **2008**, *48* (2), 378−391.
(35) Liu, H.; Hsieh, Y.-L. Ultrafine fibrous cellulose membranes from electrospinning of cellulose acetate. *J. Polym. Sci., Part B: Polym. Phys.* **2002**, *40* (18), 2119−2129.
(36) Moon, R. J.; Martini, A.; Nairn, J.; Simonsen, J.; Youngblood, J. Cellulose nanomaterials review: structure, properties and nanocomposites. *Chem. Soc. Rev.* **2011**, *40* (7), 3941.
(37) Dobosz, K. M.; Kuo-Leblanc, C. A.; Bowden, J. W.; Schiffman, J. D. Robust, Small Diameter Hydrophilic Nanofibers Improve the Flux of Ultrafiltration Membranes. *Ind. Eng. Chem. Res.* **2021**, *60* (25), 9179−9188.
(38) Kolewe, K. W.; Dobosz, K. M.; Rieger, K. A.; Chang, C.-C.; Emrick, T.; Schiffman, J. D. Antifouling Electrospun Nanofiber Mats Functionalized with Polymer Zwitterions. *ACS Appl. Mater. Interfaces* **2016**, *8* (41), 27585−27593.
(39) Schneider, C. A.; Rasband, W. S.; Eliceiri, K. W. NIH Image to ImageJ: 25 years of image analysis. *Nat. Methods* **2012**, *9* (7), 671−675.
(40) Kopeć, M.; Spanjers, J.; Scavo, E.; Ernens, D.; Duvigneau, J.; Julius Vancso, G. Surface-initiated ATRP from polydopamine-modified TiO2 nanoparticles. *Eur. Polym. J.* **2018**, *106*, 291−296.
(41) Dreyer, D. R.; Miller, D. J.; Freeman, B. D.; Paul, D. R.; Bielawski, C. W. Elucidating the Structure of Poly(dopamine). *Langmuir* **2012**, *28* (15), 6428−6435.
(42) Ding, Y.; Weng, L.-T.; Yang, M.; Yang, Z.; Lu, X.; Huang, N.; Leng, Y. Insights into the Aggregation/Deposition and Structure of a Polydopamine Film. *Langmuir* **2014**, *30* (41), 12258−12269.
(43) Dobosz, K. M.; Kuo-Leblanc, C. A.; Martin, T. J.; Schiffman, J. D. Ultrafiltration Membranes Enhanced with Electrospun Nanofibers Exhibit Improved Flux and Fouling Resistance. *Ind. Eng. Chem. Res.* **2017**, *56* (19), 5724−5733.
(44) Choong, L. T.; Yi, P.; Rutledge, G. C. Three-dimensional imaging of electrospun fiber mats using confocal laser scanning microscopy and digital image analysis. *J. Mater. Sci.* **2015**, *50* (8), 3014−3030.
(45) Getman, M.; Webber, J.; Bowser, S. An examination of MCE filter morphology and implications on preparation and analysis of air samples for asbestos. *J. Occup. Environ. Hyg.* **2017**, *14* (9), D140−D144.
(46) *Filter, MCE, 0.8 μm, 37 mm*. https://www.zefon.com/filter-mce-08m-37mm-plain-white-100pk (accessed 2021-10-21).
(47) Gibson, P.; Schreuder-Gibson, H.; Rivin, D. Transport properties of porous membranes based on electrospun nanofibers. *Colloids Surf., A* **2001**, *187−188*, 469−481.
(48) Srikrishnarka, P.; Kumar, V.; Ahuja, T.; Subramanian, V.; Selvam, A. K.; Bose, P.; Jenifer, S. K.; Mahendranath, A.; Ganayee, M. A.; Nagarajan, R.; Pradeep, T. Enhanced Capture of Particulate Matter by Molecularly Charged Electrospun Nanofibers. *ACS Sustainable Chem. Eng.* **2020**, *8* (21), 7762−7773.
(49) Al-Attabi, R.; Dumée, L. F.; Schütz, J. A.; Morsi, Y. Pore engineering towards highly efficient electrospun nanofibrous membranes for aerosol particle removal. *Sci. Total Environ.* **2018**, *625*, 706−715.
(50) Barhate, R.; Ramakrishna, S. Nanofibrous filtering media: Filtration problems and solutions from tiny materials. *J. Membr. Sci.* **2007**, *296* (1−2), 1−8.
(51) Qin, X.-H.; Wang, S.-Y. Filtration properties of electrospinning nanofibers. *J. Appl. Polym. Sci.* **2006**, *102* (2), 1285−1290.
(52) Wang, C.-S. Electrostatic forces in fibrous filters—a review. *Powder Technol.* **2001**, *118* (1−2), 166−170.
(53) Podgórski, A.; Bałazy, A.; Gradoń, L. Application of nanofibers to improve the filtration efficiency of the most penetrating aerosol particles in fibrous filters. *Chem. Eng. Sci.* **2006**, *61* (20), 6804−6815.
(54) Ryu, J. H.; Messersmith, P. B.; Lee, H. Polydopamine Surface Chemistry: A Decade of Discovery. *ACS Appl. Mater. Interfaces* **2018**, *10* (9), 7523−7540.
(55) Zhao, X.; Li, Y.; Hua, T.; Jiang, P.; Yin, X.; Yu, J.; Ding, B. Cleanable Air Filter Transferring Moisture and Effectively Capturing PM2.5. *Small* **2017**, *13* (11), 1603306.

https://doi.org/10.1021/acs.iecr.1c03051
Ind. Eng. Chem. Res. XXXX, XXX, XXX−XXX

Optimizing the Packing Density and Chemistry of Cellulose Nanofilters for High-Efficiency Particulate Removal

Shao-Hsiang Hung[1], Jared W. Bowden[1], Richard E. Peltier[2], and Jessica D. Schiffman[1*]

[1]Department of Chemical Engineering, University of Massachusetts Amherst, Amherst, Massachusetts 01003-9303, United States

[2]School of Public Health & Health Sciences, University of Massachusetts Amherst, Amherst, Massachusetts 01003-9303, United States

* Corresponding author: Jessica D. Schiffman

Email: schiffman@ecs.umass.edu; Phone: (413) 545-6143

Table S1. Summary of the elemental data analysis of the high resolution XPS that provides surface chemical composition analysis of cellulose, PDA, and PDADMAC electrospun nanofilters.

Nanofilter	C (%)	O (%)	N (%)
Cellulose	59.1	38.6	0.1
PDA	64.0	33.4	2.5
PDADMAC	65.8	31.5	1.5

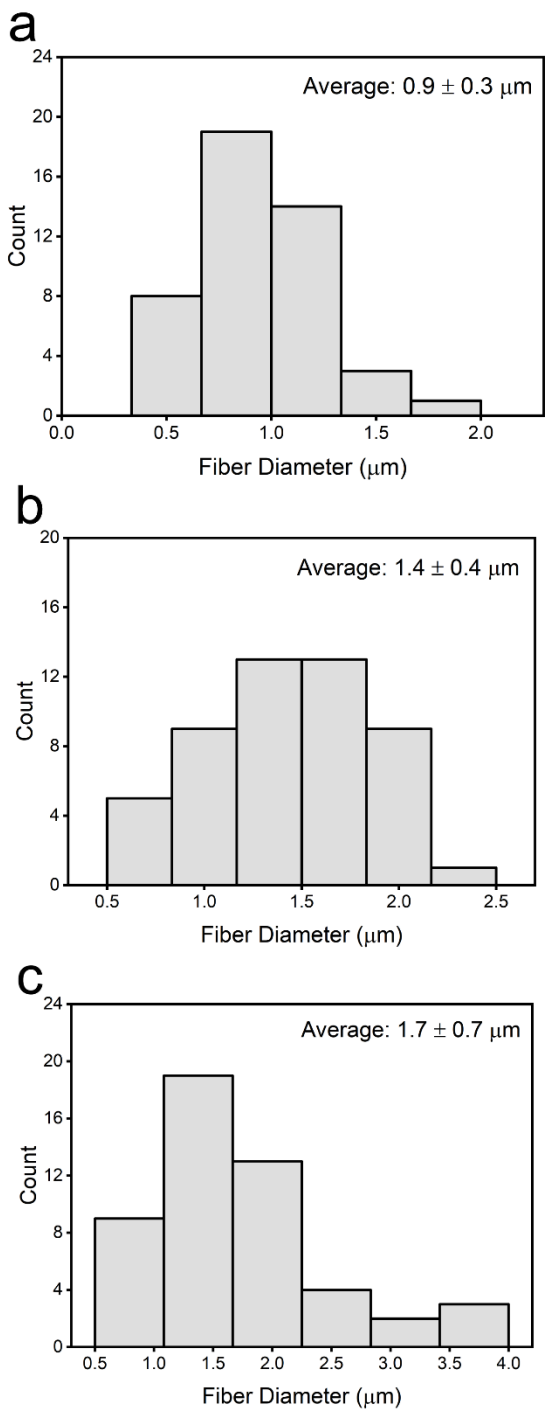

Figure S1. Fiber diameter distribution and average fiber diameter of (a) cellulose (b) PDA-functionalized, and (c) PDADMAC-functionalized nanofilters.

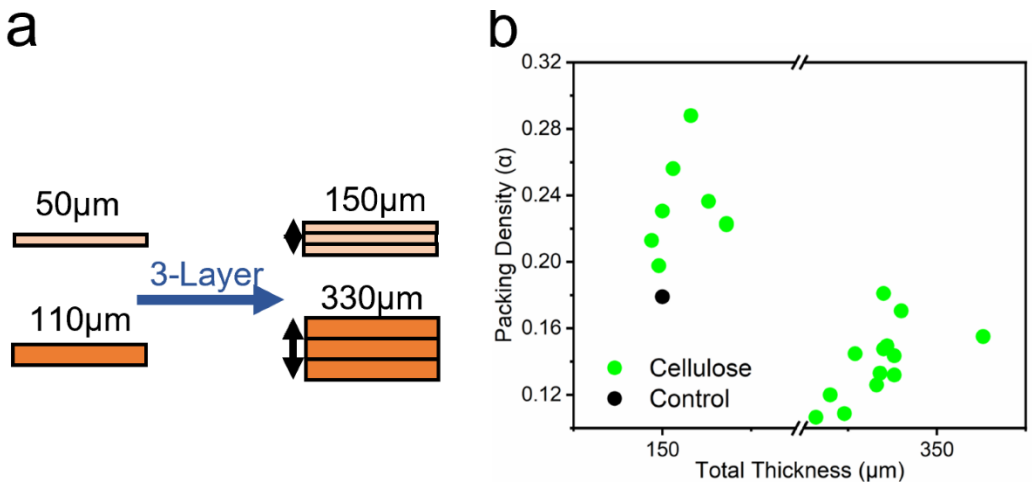

Figure S2. (a) Schematic diagram of single and multilayer electrospun nanofilters with different thicknesses. (b) Packing density as a function of total thickness for MCE controls and all cellulose nanofilters investigated in this work.

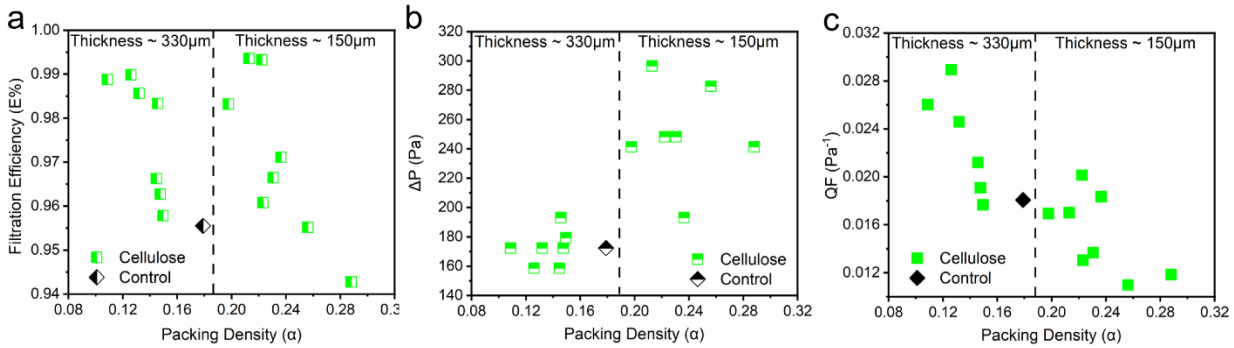

Figure S3. (a) Filtration efficiency (b) Pressure drop and (c) Quality factor as a function of packing density for the MCE control, and cellulose nanofilters. The dotted line separates the filters that had a total bulk thickness of 330 μm from those that were 150 μm thick.

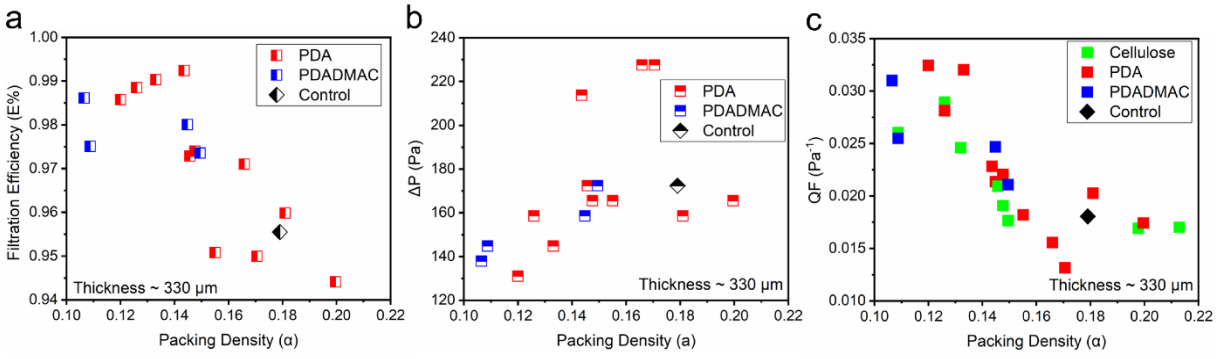

Figure S4. (a) Filtration efficiency (b) Pressure drop and (c) Quality factor as a function of packing density for the MCE control, PDA and PDADMAC samples. All samples had a total filter thickness of 330 μm.